

# Preliminary Result of ALOS/PALSAR Fully Polarimetric Data and its Comparison with Pi-SAR Data

#Xu Xin<sup>1</sup>, Yoshio Yamaguchi<sup>1</sup>, Yuki Yajima<sup>1</sup>, Hiroyoshi Yamada<sup>1</sup>

<sup>1</sup>Dept. of information Engineering, Niigata University  
Ikarashi 2-8050, Niigata-shi, 950-2181 Japan, xuxin@wave.ie.niigata-u.ac.jp

## 1. Introduction

The Advanced Land Observing Satellite (ALOS) was successfully launched on Jan. 24, 2006, from Tanegashima Space Center, Japan. The objectives of ALOS are [1]:

- (1) to provide maps for Japan and other countries including Asia-Pacific region (Cartography),
- (2) to perform regional observation for "sustainable development", harmonization between Earth environment and development (Regional Observation),
- (3) to conduct disaster monitoring around the world (Disaster Monitoring),
- (4) to survey natural resources (Resources Surveying),
- (5) to develop technology necessary for future Earth observing satellite (Technology Development).

It enhances land observation technologies acquired through the development and operation of its predecessors, the Japanese Earth Resource Satellite-1 (JERS-1) and the Advanced Earth Observing Satellite (ADEOS). ALOS is one of the largest earth observing satellites ever developed.

In this paper, a preliminary result of the fully polarimetric data is presented. The fully polarimetric data from space-borne Synthetic Aperture Radar (SAR) is the first one in the world. Using the four-component decomposition algorithm [2] based on the coherency matrix, the polarimetric data are decomposed and are compared with Pi-SAR (an airborne SAR) data set. Fig. 1 shows ALOS in space. Fig. 2 shows the operation mode of PALSAR.



Figure 1: ALOS in space

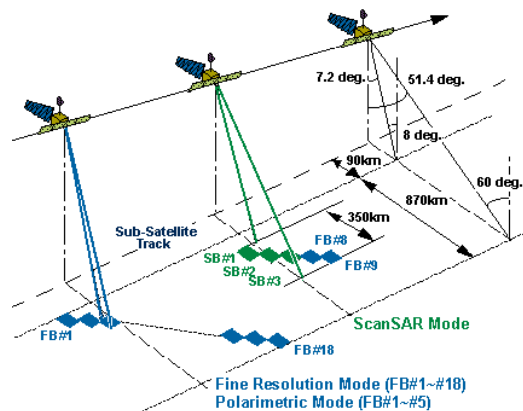


Figure 2: Operation mode of PALSAR [1]

## 2. Four-component Decomposition Algorithm

This method decomposes the total scattering power into surface scattering power  $P_s$ , double bounce scattering power  $P_d$ , volume scattering power  $P_v$ , and helix scattering power  $P_c$  (Fig. 3). It enables us to find scattering mechanism of the terrain, which serves to classify and identify target in POLSAR image. The detail of the decomposition algorithm is shown in ref. [2].

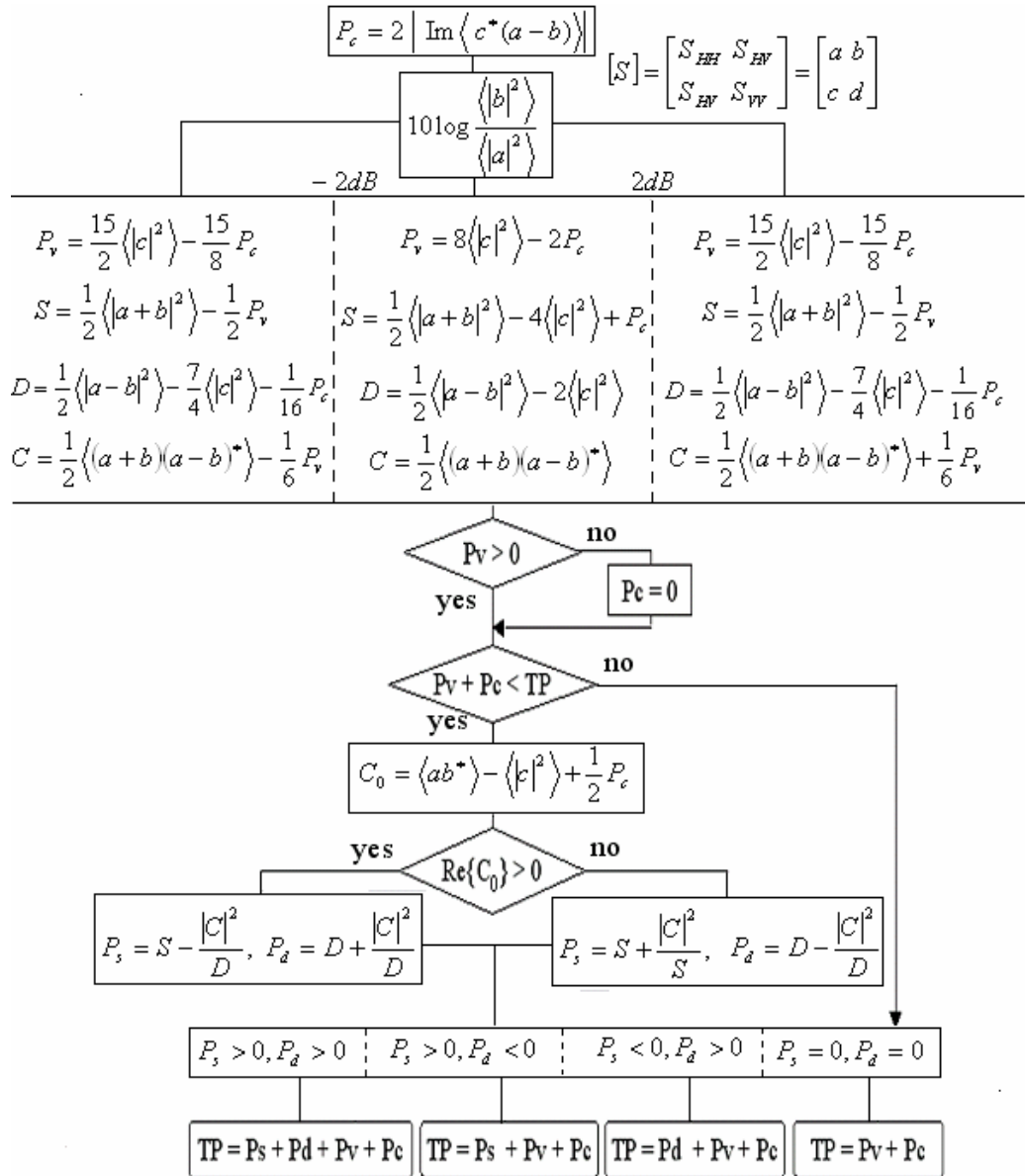


Figure 3: Modified algorithm of four-component decomposition algorithm amended by power constraints

### 3. Decomposed results of ALOS/PALSAR and Pi-SAR Data

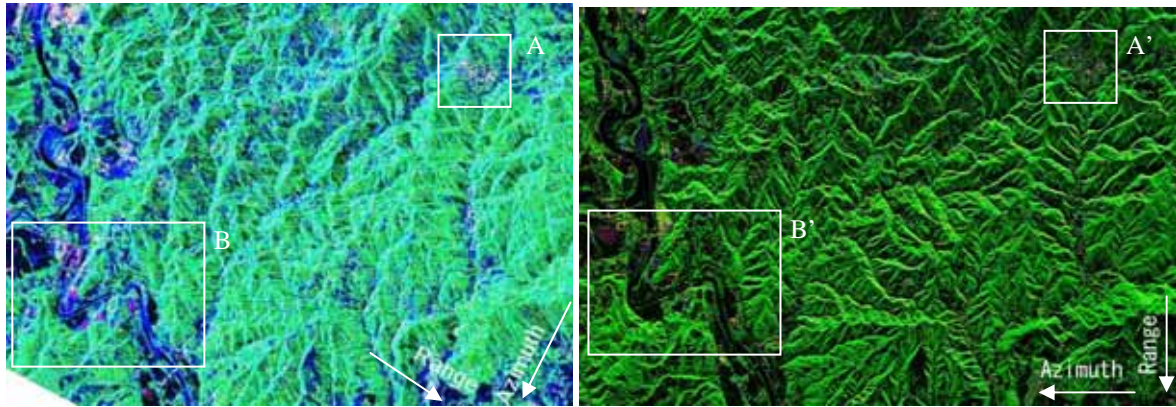
We applied the four-component decomposition algorithm to the dataset acquired with ALOS/PALSAR polarimetric mode and an airborne Pi-SAR system. Since both of them provide fully polarimetric data, the decomposition as well as their comparison becomes available. The data sets have been acquired by ALOS/PALSAR (June, 2007) and Pi-SAR (Oct. 26, 2004).

The color-coded decomposed images are shown in Fig.4 for the sake of comparison. The color-composite consists of Red ( $P_d$ ), Green ( $P_v$ ), and Blue ( $P_s$ ). Since the radar illumination direction and the incidence angle are different, one can see the images look like different each other although the same area has been observed. In addition, the ground range resolution of PALSAR is 20 m by 30 m, whereas the resolution of Pi-SAR is 3 m by 3 m. This leads to fine resolution in Pi-SAR image.

It is seen in PALSAR image that Green ( $P_v$ ) dominates whole area and Blue ( $P_s$ ) can be seen around river in the left corner of the image. The Blue ( $P_s$ ) seems to be caused by the incidence angle of 24 degrees of ALOS/PALSAR polarimetric mode. A small incidence angle yields single

bounce scattering dominantly compared to double bounce scattering. On the other hand, Pi-SAR image is covered with Green ( $P_v$ ) predominantly. This is caused by volume scattering with the incidence angle of 34-40 degrees.

Since the area is too large for the analysis, we have chosen two specific areas, Yamakoshi village and Kawaguchi-machi, suffered from a great earthquake on Oct. 23, 2004.



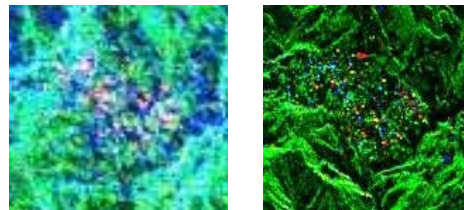
ALOS/PALSAR

Pi-SAR (L-band)

Figure 4: Color-coded decomposed images of ALOS/PALSAR and Pi-SAR over Chuetsu earthquake region: Red ( $P_d$ ), Green ( $P_v$ ), Blue ( $P_s$ ).

### 3.1 Yamakoshi area

Fig.5 shows close-up images of the boxes A in Fig.4. The area is Tanesuhara, Yamakoshi village, where residential houses are located. A lot of red or yellow points can be recognized in the center of Pi-SAR image. Red ( $P_d$ ) represents double bounce scattering caused by residential houses. On the other hand, corresponding points are White in PALSAR image. This White means that the powers  $P_s$ ,  $P_d$ , and  $P_v$  are approximately the same. This seems be caused by the  $P_s$  behavior with respect to the incidence angle, i.e.,  $P_s$  is stronger in smaller incidence angles.



ALOS-PALSAR

Pi-SAR

Figure 5: Close-up images of the box A in Fig.4.

### 3.2 Kawaguchi-machi area

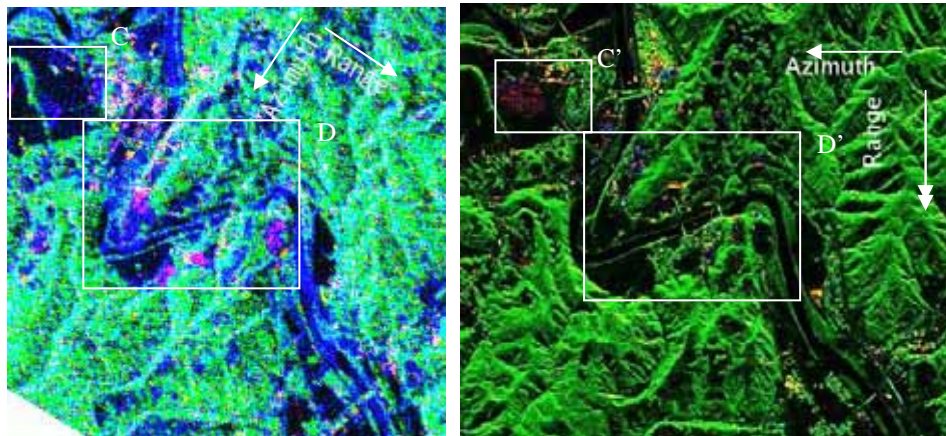
The next study area is Kawaguchi-machi area. Fig.6 shows close-up images of the box B in Fig.4. In addition, Fig.7 shows the optical image of the same area for comparison.

If we compare the portion on the left top corner (marked by the square C', rice paddy field) of Pi-SAR image with the optical one, a great difference between PALSAR and Pi-SAR can be seen. The double scattering power  $P_d$  is strong in Pi-SAR, whereas the surface scattering  $P_s$  is stronger in PALSAR. This result is consistent with the scattering property that double bounce from a dihedral corner reflector is relevant to the azimuth angle. In this case, bunches of rice construct dihedral corner reflector structure and its orientation is orthogonal to the Pi-SAR illumination.

Polarimetric scattering characteristics of another type (red areas in ALOS/PALSAR) can be seen in the box D at center of the images.

## 4. Conclusions

A four-component decomposition of scattering powers was applied to the Pi-SAR and ALOS/PALSAR fully polarimetric data set in the L-band. The four-component decomposition using the coherency matrix seems effective for extracting physical scattering nature. By comparing the difference of  $P_s$ ,  $P_d$  and  $P_v$  scattering terms in the two images, the decomposition results seem appropriate as regards the different incidence angles and oriented directions. Since a lot of fully polarimetric data become available, it is necessary to carry out data analysis and make use of the data for environmental research such as disaster monitoring, land classification, polarimetric interferometry for land slide detection, etc.



ALOS-PALSAR Pi-SAR  
Figure 6: Close-up images of the box B in Fig.4

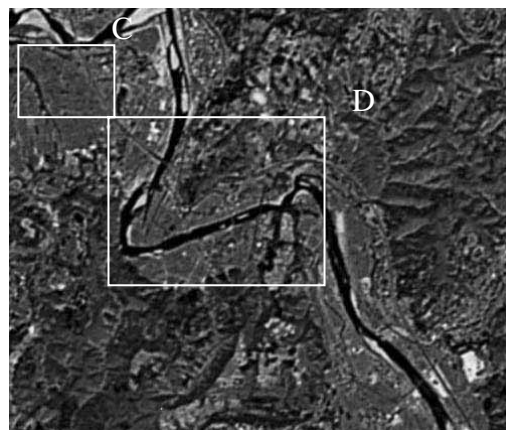


Figure 7: Optical image of Kawaguchi area

## Acknowledgment

The authors are grateful to Pi-SAR data provided by NICT and JAXA, Japan, and ALOS/PALSAR data provided by ERSDAC, Japan.

## References

- [1] <http://www.eorc.jaxa.jp/ALOS>
- [2] Y. Yamaguchi, Y. Yajima, and H. Yamada, "A four-component decomposition of POLSAR images based on the coherency matrix," *IEEE Geoscience Remote Sensing Letters*, vol.3, no.3, pp.292-296, 2006
- [3] A. Freeman, and S. L. Durden, "A three-component scattering model for polarimetric SAR data," *IEEE Trans. Geoscience Remote Sensing*, vol.36, no.3, pp.936-973, May 1998